Modern Environmental Science and Engineering (ISSN 2333-2581)
October 2020, Volume 6, No. 10, pp. 1150-1154
Doi: 10.15341/mese(2333-2581)/10.06.2020/015
Academic Star Publishing Company, 2020
www.academicstar.us

Determination of Total Nitrogen and Phosphorus in a Reservoir by Remote Monitoring of a Drone and Calibrated Empirical Equations, Lima, Perú

Daniel Antonio Caballero Beltran, Evelyn Estefany Melgar Támara, and Ricardo Fernando León Ochoa
Universidad Nacional Agraria La Molina, Lima, Perú

Abstract: The irrigation reservoir Unit of Universidad Nacional Agraria La Molina receives water from the Rimac river for irrigation purposes. While Rimac River has a large source of pollution along its 127 km of riverbed from discharges, mainly domestic, industrial and mining waste, so there is a high probability of eutrophication, being necessary and very important the monitoring of nitrogen and total phosphorus for a better control. For this purpose, monitoring was proposed with the planning of the flight path (app DJI) and image acquisition with a multispectral camera (Sentera) coupled to an RPA (drone, Phamton 3 Advance) in order to acquire a cloud of images, RGB and NIR (Near-infrared), for the generation of a multispectral mosaic and its modeling through empirical equations and raster tools. The final product was thematic maps of the Total Phosphorus and Total Phosphorus levels in the reservoir whose digital levels of maps were compared with samples obtained from the reservoir, reaching a high degree of chi-square correlation equal to 0.94; to finally calibrate the empirical equations and get a general equation of greater precision and representative maps of the Total Nitrogen (NT) and Total Phosphorus (TF) levels of the reservoir, which future monitoring can be performed in shorter time periods these indices.

Key words: water quality monitoring, remotely piloted aircraft system (RPAS), remote sensing, modeling

1. Introduction

At present, the challenge of the water resource problem at world-wide is gaining greater relevance in all researches, and one of the main issues revolves around the process of eutrophication, associated mainly with the parameters of NT and FT, a problem that has led to an accelerated loss of water bodies due to pollution and subsequent disappearance. This problem is a consequence of human activities that introduce an excess of nutrients [1], being defined as a process of deterioration of the quality of the resource and is caused by the enrichment of nutrients [2].

Water quality monitoring is the first step towards understanding the characteristics of water pollution and developing effective mitigation strategies. Traditionally, water quality parameters such as Total Nitrogen (TN) and Total Phosphorus (TP) are obtained through routine monitoring methods of field sampling and laboratory analysis [3]. However, the development of remote sensing has had a key impact on monitoring because of the advantages it offers [4]. Currently, sensors on satellites that have a large number of spectral, spatial and temporal resolutions have been used to access various water quality parameters [3] and are available in various resolutions with very similar characteristics, allowing them to be mounted on Unmanned Aerial Vehicles or Remote Pilot Aircraft (RPA), having as main advantage as higher resolution. [5].

Corresponding author: Daniel Antonio Caballero Beltran, Bachelor; research areas/interests: remote sensing, hydrology and environment engineering. E-mail: daniel_caball@outlook.com.

For all the above reasons mentioned, this research proposes the use of high-resolution remote sensing with multispectral sensors coupled to UAVs-RPA for monitoring water quality parameters, NT and FT, related to eutrophication.

2. Material and Methods

The experimental work was an applied research, carried out in the "Reservoir of the Unit of Technified Irrigation-UNALM" in association with the Technified Irrigation Unit of the National Agrarian University La Molina, owner of the reservoir. The following materials were used for information gathering: Multispectral camera (Sentera) fixed to the RPA (drone, Phamton 3 Advance), and a drone pilot with RPAS Transitory Operator Accreditation issued by the Civil Aeronautical Director (DGAC). The equipment for collecting water samples from the reservoir followed a water monitoring protocol for subsequent laboratory analysis. The equipment consisted of sampling containers, a thermally insulated box and neutral samples, winches and nylon cord for sampling and georeferencing. For photogrammetric processing, the Pix4D software was used, generating reflectance maps.

A data collection campaign was carried out, where water samples were taken at three points, collected in 1L high density polyethylene containers, stored in a thermo-insulated box and sent to the UNALM Agua, suelo, medio ambiente y fertirriego Laboratory for NT and FT analysis. Finally, the sampling points were georeferenced in a GIS software.

For the reflectance maps, a return was made at a height of 50 meters, taking into account a ground sample distance (GSD) of approximately 3cm, the information survey (photo cloud) was processed in the Pix4D Mapper software, from which the reflectance maps in the Red, Green, Blue (RGB) and Near Infrared Red (NIR) bands were exported. The reflectance maps of the different bands were loaded into the Arcgis software, where the sampling points were also loaded (Fig. 3), and reflectance values were taken from the different bands in the area of location of each sampling point (Table 2).

The extracted reflectance values (Table 2) were compared with the values of the concentration level points of NT and FT (Table 1), seeking in this way a correlation between them. For this purpose, cases constituted by sets of inputs and outputs will be entered where the input data will be the reflectance of the different bands and the output data will be the concentration levels of NT and FT separately., so that the most appropriate relationship, either linear or exponential, will be found according to the determination of coefficient R Square.

Table 1 Laboratory data results and location of points.

Sampling label		Parameters (mg/l)		Geographic location			
		T. Phosphorus	T. Nitrogen	Latitude	Longitude	East	North
5051	Point1	1.66	1.55	-12.078911	-76.941149	288712.818	8663971.34
5020	Point 2	1.09	3.1	-12.078682	-76.940937	288735.722	8663996.84
5010	Point 3	2.03	5.17	-12.078723	-76.940587	288773.864	8663992.57

Table 2 Total nitrogen, total phosphorus levels and reflectance data from different bands at different sampling points.

Points	Parameters (mg/l)		Reflectance in different bands			
	T. Phosphorus	T. Nitrogen	Red	Green	Blue	NIR
1	1.66	1.55	53	60	57	35.7
2	1.09	3.1	94	99	91	29
3	2.03	5.17	93	104	98	20.7

3. Results and Discussion

The relationship between the values of Reflectance and NT and FT concentrations can be seen in Tables 3 and 4, observing for the case of NT (Table 3) the values of reflectance of each band and values of NT concentration are better suited to the case of a linear Regression, having values of R2 of 0.99 in the NIR band and R2 of 0.66 in the Red band, this strong relationship between the NIR band and the content of NT in a water body can be observed in studies made with satellite images [6]; for the case of the FT (Table 4), we present low values of R2 in the relation of the concentration levels with the reflectance values of the bands, having as the best value of 0.2 of R2 for the Linear regression of the NIR Band and as the lowest value of 0.0003 of R2 in the case of the Green Band, this tendency to lower relation with the case of NT can already be observed in prior works [4].

It can be seen in Fig. 1 the spatial distribution of FT, that all values are low with points less than 0.523 kg/l, observing a uniformity throughout the reservoir length. Also, it should be emphasized the location of the sampling points (Fig. 3) does not coincide with the samples produced by the laboratory (Table 1), this is due to the low correlation coefficient R2 in the

Table 3 R2 values based on the regression used for total nitrogen values.

Band	R2 Values	
	Linear Regression	Exponential Regression
Red	0.66	0.81
Green	0.77	0.89
Blue	0.81	0.92
NIR	0.99	0.97

Table 4 R2 values based on the regression used for total phosphorus values.

Band	R2 Values	
	Linear Regression	Exponential Regression
Red	0.02	0.05
Green	0.0003	0.01
Blue	0.0014	0.002
NIR	0.2014	0.14

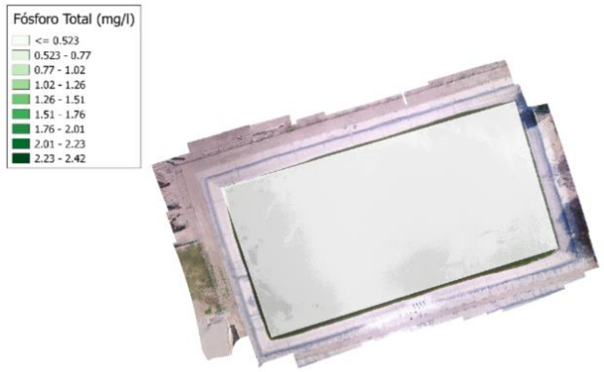

Fig. 1 Total phosphorous spatial distribution – Graphic 3 equation.

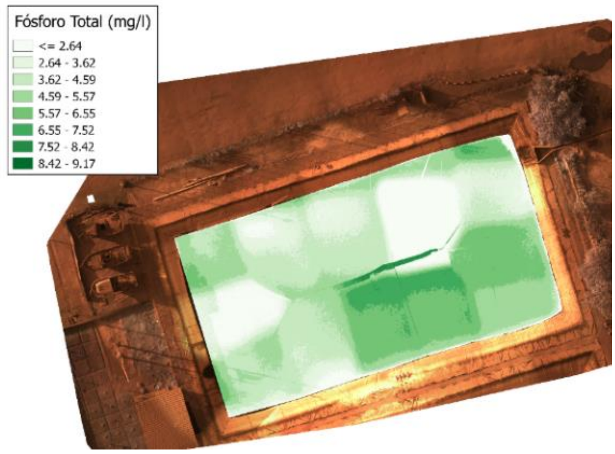

Fig. 2 Total nitrogen spatial distribution – Graphic 1 equation.

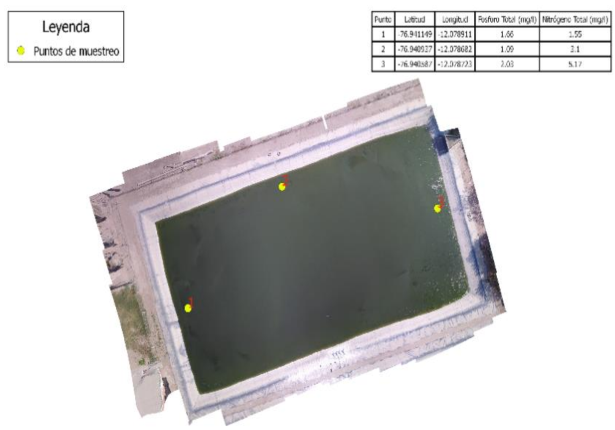

Fig. 3 RGB reservoir and points location sample.

equation used (Fig. 2); unlike the map of Total Nitrogen distribution (Fig. 2), this one attends a varied distribution of Total Nitrogen concentration, observing a slightly higher concentration in the central zone of the

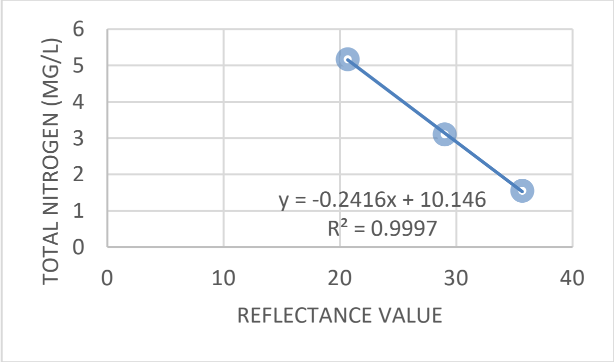

Graph 1 Total nitrogen vs NIR band.

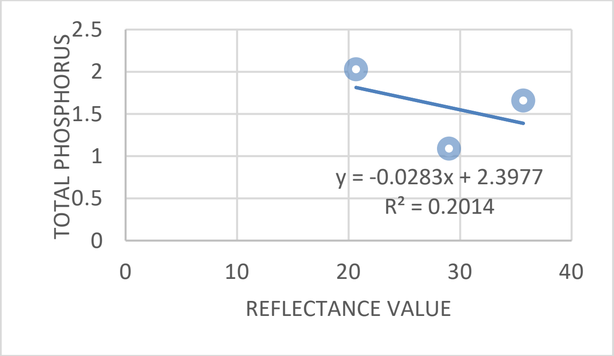

Graph 2 Total phosphorus vs NIR band.

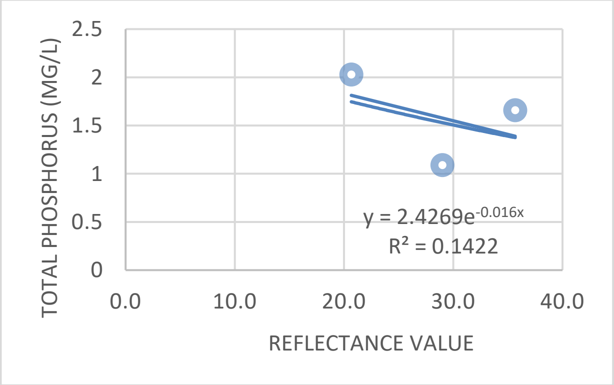

Graph 3 Total phosphorus vs NIR band.

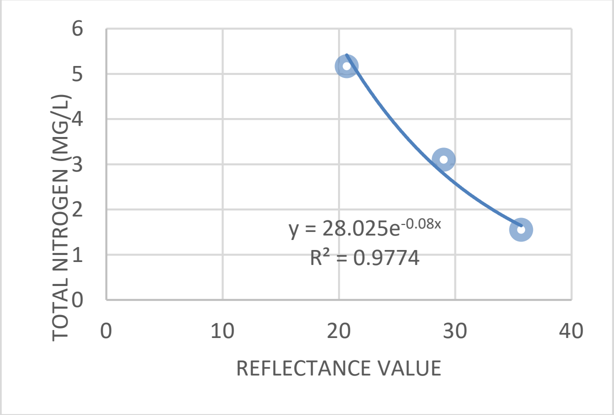

Graph 4 Total Nitrogen vs NIR Band.

reservoir, this distribution map does present coincidences in the laboratory sampling zones, and this is largely due to the fact that the equation used presents a high R2 correlation coefficient of 0. 99 (Graph 1).

4. Conclusion

The determination of NT and FT concentrations in the UNALM URT reservoir with high resolution sensors was developed by comparing linear and exponential models of the reflectance values of the Red, Green, Blue (RGB) and Infrared (Near) bands that were used to establish a relationship with the concentrations of NT and FT that were collected and analyzed in the laboratory; the trend of these two models is similar to those obtained in other similar studies, supporting their applicability and validity. The results of the FT model, present tendencies to improve with a greater amount of samples, these can reach high levels of correlation coefficient as seen in studies such as those of Liu et al., 2015, which obtained values of 0.94 for FT. Linear and exponential models have relatively simple forms and only require a single band to calculate NT and FT concentrations.

The spatial distribution maps (Fig. 1 and Fig. 2) allow us the interpretation of the spatial patterns of NT and FT in the whole reservoir area; in the case of the Spatial Distribution of NT (Fig. 2), the water quality conditions coincide with the samples taken to the laboratory, working only with the NIR Band. Therefore, the results of this study indicate the feasibility of monitoring the concentrations of TL in static water bodies such as the reservoir under study with high-resolution sensors fixed in a drone, these maps will be used to assist in decision making in relation to improving water management identify challenges for targeted decision making.

This study presents a technical potential of images from the Sentera sensor to estimate NT concentrations in water bodies. Further studies are needed to examine the determination of contaminants from multispectral data from RPA-mounted sensors over the study area and other water bodies. In this study, only 3 sample points are used (Table 1), therefore, also the low value of correlation coefficient R2 in the case of Total Phosphorus, being necessary to make more experiences using a higher amount of sample data can be useful to consolidate these conclusions.

The concentrations of NT and FT, in static water bodies, have an indirect relationship with the optical properties of the water, which supports the development of additional work with a greater number of samples and using neural networks, which presents relationship algorithms in constituted cases, with input and output values, which would find a relationship for a greater degree of options when finding the relationship between the values of reflectance and those of concentration of NT and FT.

References

[1] J. Neiber, Energieeinsparung und Lastmanagement, C.A.R.M.E.N.-Forum, 2013, pp. 59-67.

[2] S. Neser, J. Neiber and K. Bonkoß, Stromverbrauch und Energieeffizienz, *Schule und Beratung* 11 (2012) 7-12.

[3] AEL e.V., Effizienter Stromeinsatz, available online at: http://www.ael-online.de/inhalt/fachinfo/download/tipps.

[4] J. Neiber and S. Neser, Energysaving potentials, *Landtechnik* 65 (2010) 421-425.

[5] DIN 18910, Wärmeschutz geschlossener Ställe, Deutsches Institut für Normung e.V., 2004.

[6] H. Eckel, W. Büscher, B. Feller, S. Fritzsche, Ch. Gaio, H. Kämper and J. Neiber, Energiebedarf, KTBL-Heft 105, 2014.

[7] C. Seifert, D. Wietzke and S. Fritzsche, Heizung und Lüftung, *Landtechnik* 64 (2009) 423-425.

[8] H. J. Kruczek, H. Kämper, G. Scheibe, B. Feller, N. Lohmann, W. Büscher, G. Schmitt-Pauksztat, T. Schneider and S. Schierhold, Planungsdaten, *KTBL-Schrift* 445 (2005) 19-52.

[9] P. Pommer, H. Eckel, W. Hartmannand H. Kämper, Energie in der Milchviehhaltung, *KTBL-Heft* 104 (2014).

[10] A. Fübbecker, Stromeinsparung, LWK Niedersachsen, available online at: http://www.lwk-niedersachsen.de/index.cfm/portal/6/nav/1082/article/17834.html, 2011.

[11] Bay. StMWi, Energie-Atlas, available online at: http://www.energieatlas.bayern.de/index.html.

[12] J. Neiber and W. Schmid, Saving potential, *PV-Magazine* 3 (2013) 79-83.